Supporting Information (SI)

Continuous and Inexpensive Monitoring of Non-Purgeable Organic Carbon by Coupling High-Efficiency Photo-oxidation Vapor Generation to Miniaturized Point Discharge Optical Emission Spectrometry

Shu Zhang[1], Yunfei Tian[3], Hongling Yin[2], Yubin Su[1], Li Wu[3], Xiandeng Hou[1,3], and Chengbin Zheng[1*]

[1] Key Laboratory of Green Chemistry & Technology of MOE, College of Chemistry, Sichuan University, Chengdu, Sichuan 610064, China

[2] College of Resources and Environment, Chengdu University of Information Technology, Chengdu 610225, China

[3] Analytical & Testing Center, Sichuan University, Chengdu, Sichuan 610064, China

*Corresponding author:

Fax: +86 28 85412907; Phone: +86-28-85415810

E–mails: abinscu@scu.edu.cn (C. B. Zheng)

Table of Contents

1. **PD-OES**
2. **DBD-OES**
3. **Picture of FI-HE-POVG-PD-OES**
4. **The Full Instrumental Setup of Continuous HE-POVG-PD-OES**
5. **Sampling Map**
6. **Sample Preparation**
7. **Optimization of UV-POVG-PD-OES Experimental Conditions**
8. **The Oxidation Efficiencies of Humic Acids, NPOC of Real Water and KHP**
9. **Interferences**
10. **Precision**
11. **Comparison of Performance with Other Methods**
12. **Calibration Curve Obtained by Using Continuous HE-POVG-PD-OES**
13. **The Picture of Continuous and Continuous Monitoring of NPOC in Tap Water**

1. PD-OES.

The experimental setup of PD-OES is same with that reported in our previous work. Briefly, it mainly consists of a PD excitation source and a commercial hand-held charge coupled device (CCD) spectrometer (Maya 2000 Pro, Ocean Optics Inc., Dunedin, FL, USA) retaining 0.4 nm of spectral resolution and a 200-400 nm of spectral range. The PD excitation source consists of two tapered tungsten electrodes and a polytetrafluoroethylene (PTFE) chamber (1.0 cm length × 0.8 cm i.d. × 2.2 cm o.d.). The discharge microplasma will be generated when these electrodes were supplied power from a compact ac neon sign electron transformer power supply (NGB408BL, Electronic Equipment Factory of Jinshi, Guangzhou, China; 14 cm long × 6 cm wide × 5 cm high, with a rated output of 8 kV, 30 kHz, and 24 W at 220 V, 60 Hz input). Optical emission from the discharge was recorded with the CCD spectrometer.

2. DBD-OES.

DBD-OES consisted of a cylindrical DBD and the miniaturized CCD Spectrometer. According to our previous work, the DBD device was made using a quartz tube (50 mm × 3.0 mm i.d. × 5.0 mm o.d.) and two separated copper wires, which served as electrodes. One was tightly wrapped around the outside of the tube evenly and used as outer electrode, the other was inserted into the tube and used as inner electrode. These electrodes were connected to the power supply used in PD-OES.

3. Picture of FI-HE-POVG-PD-OES

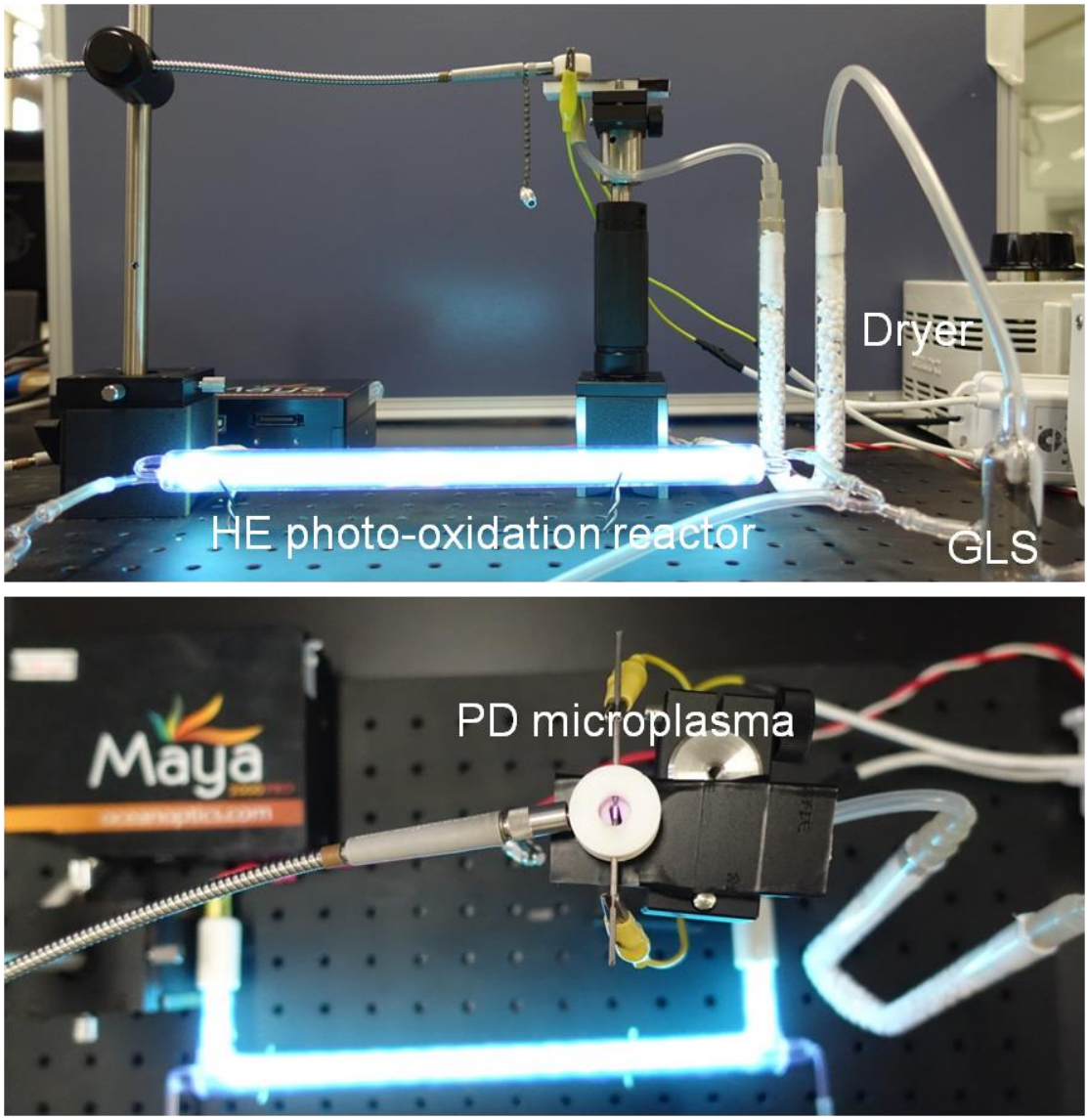

Figure S1. Picture of FI-HE-POVG-PD-OES.

4. The Full Instrumental Setup of Continuous HE-POVG-PD-OES

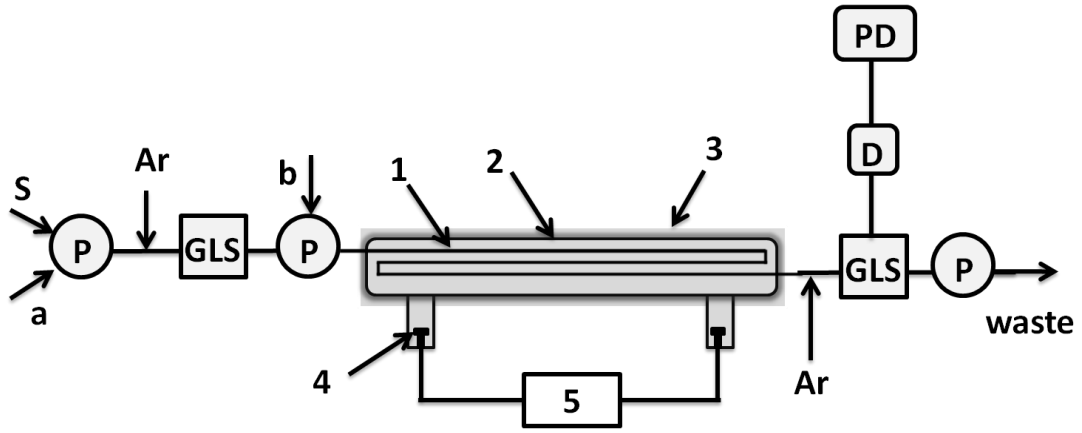

Figure S2. The instrumental setup of continuous HE-POVG-PD-OES. 1, quartz inner tube; 2, outer surface of the low-pressure mercury lamp; 3, aluminum foil; 4, electrode; 5, ballast resistor and power source; S, sample solution. a,10% phosphoric acid solution; b, sodium persulfate solution; P, pump; GLS, gas liquid separator; D, drying tube; PD, point discharge chamber.

5. **The Sampling Map**

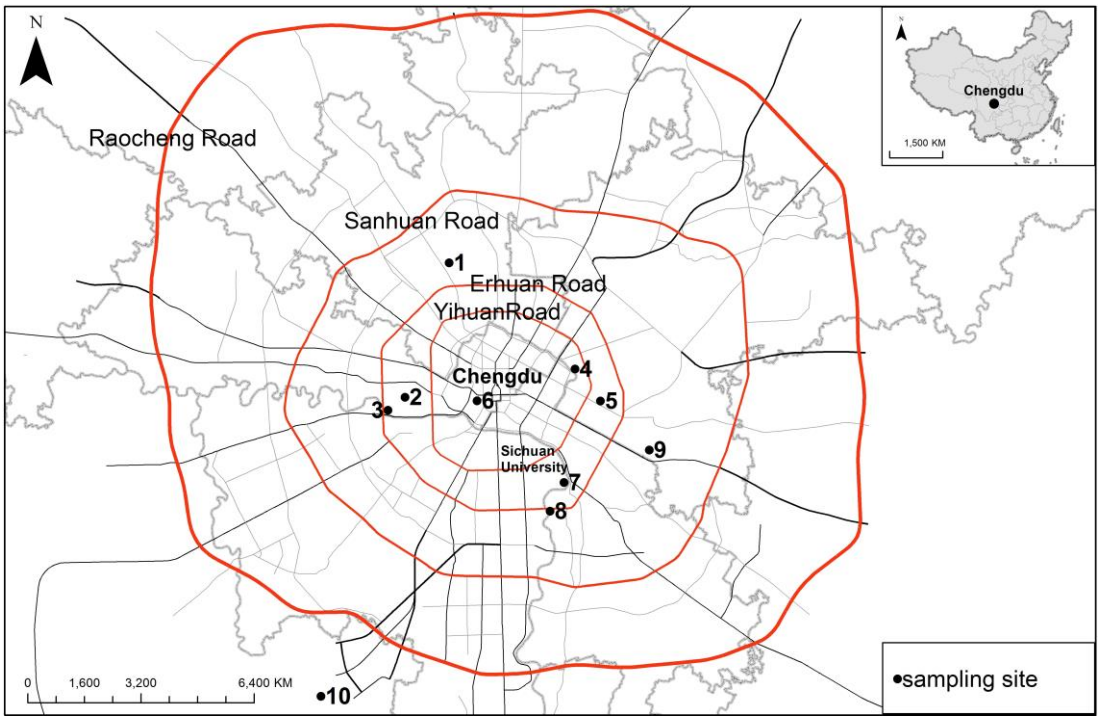

Figure S3. Sampling locations.

6. Sample Preparation

All the water samples were collected in the 250 mL glass bottles. These bottles were soaked in 0.2% (v/v) of nitric acid for 12 h and subsequently flushed with DIW for several times and finally dried before use. The collected samples were analyzed immediately after sending to the laboratory. We firstly used the 0.45 μm glass fiber filters to remove the particle substance. According to the manual instruction of analytikjena multi N/C 2100 analyzer, the samples were acidified using 10% (v/v) phosphoric acid solution and purged with 200 mL min^{-1} of argon for 3 min before analysis using the proposed system.

7. Optimization of UV-POVG-PD-OES Experimental Conditions.

As can be seen in Figure S4a, the emission intensity increased with increasing the discharge voltage before 2.85 KV and the discharge became unstable and the emission intensity decreased at higher discharge voltage. So we chose the 2.55 kV as the optimal voltage. The results summarized in Figure S4b show that the emission intensity increased obviously when the discharge gap was lower than 3 mm, followed by an obvious decrease at bigger gap. So 3 mm of discharge gap was used in subsequent experiments. In Figure S4c, when the flow rate of carrier gas was improved, the emission peak height increased whereas the peak area declined. This is because that although the higher flow rate could improve gas liquid separation efficiency, it also resulted in serious dilution of analytes. Finally, 300 mL min^{-1} of Ar carrier gas was used in the further experiments.

The effect of the flow rate of carrier solution on response was also investigated, as shown in Figure S5a. The results show that the optimum response is obtained at 3 mL min^{-1} of carrier solution. It is well known that the oxidation efficiencies of organics are dependent on the concentration of oxidant, the effect of the concentration of $Na_2S_2O_8$ was thus studied. The results (Figure S5b), the response reaches a maximum value when the concentration of $Na_2S_2O_8$ solution is higher than 300 g L^{-1}. The final conditions used for the subsequent experiments are summarized in Table S1.

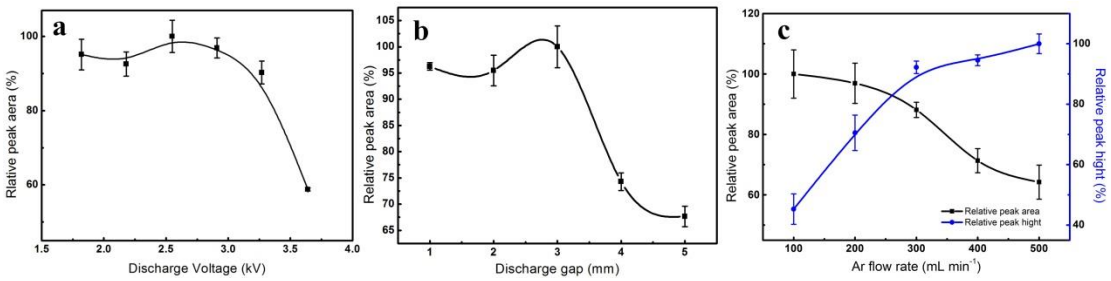

Figure S4. Effects of PD conditions on the carbon response. a, discharge voltage; b, discharge gap; c, flow rate of argon carrier.

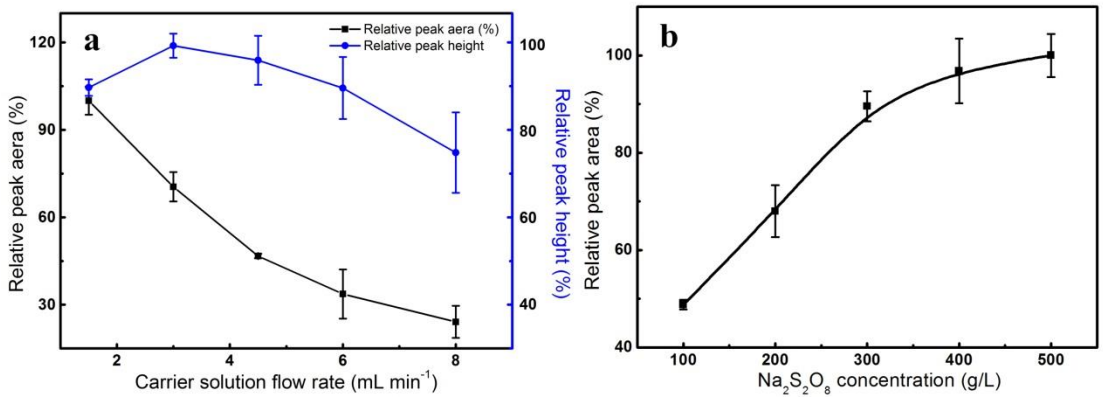

Figure S5. Effects of the photo-oxidation conditions on the carbon response. a, carrier solution f low rate; b, The concentration of $Na_2S_2O_8$ solution.

Table S1. Experimental Conditions for the Determination of NPOC by UV-POVG-PD-OES

Experiment Parameter	value
Discharge gap, mm	3
Discharge voltage, kV	2.55
Ar carrier flow rate, mL min^{-1}	300
Carrier solution flow rate, mL min^{-1}	3
$Na_2S_2O_8$ concentration, g L^{-1}	300

8. The Oxidation Efficiencies of Humic Acids, NPOC of Real Water and KHP

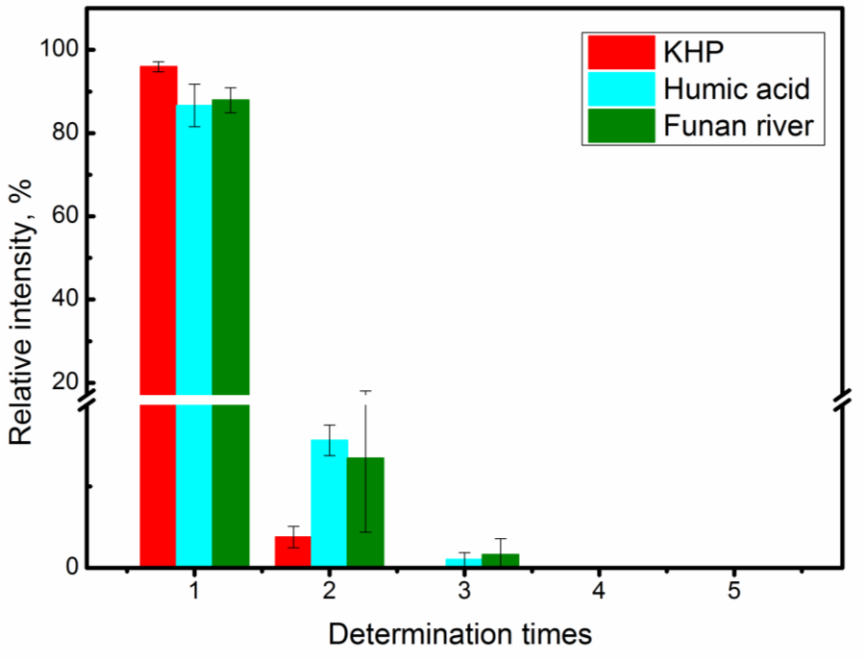

Figure S6. The oxidation efficiencies obtained from the n-th UV photo-oxidation.

9. Interferences.

Table S2. Influence of Concomitant Ions on the Determination of 10 mg L^{-1} (as C) KHP

Ions	Concentration (mg L^{-1})	Recoveries, %
Na^{+}	500	99±8
K^{+}	500	100±1
Fe^{3+}	500	91±7
Zn^{2+}	500	91±2
Mn^{2+}	500	101±3
Mg^{2+}	500	101±5
Cu^{2+}	500	95±3
Ag^{+}	500	89±6
Fe^{2+}	500	88±2
Ca^{2+}	500	88±3
PO_4^{3-}	100000	88±8
SO_4^{2}	100000	99±8
NO_3^{-}	100000	73±3
Cl^{-}	100000	65±2

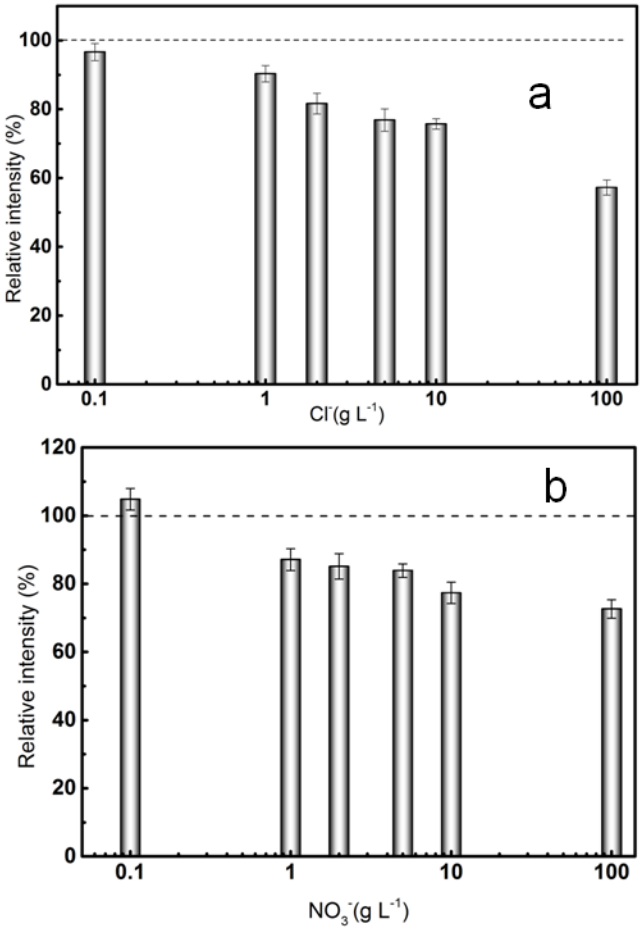

Figure S7. The interference of NO_3^- and Cl^-

10. Precision

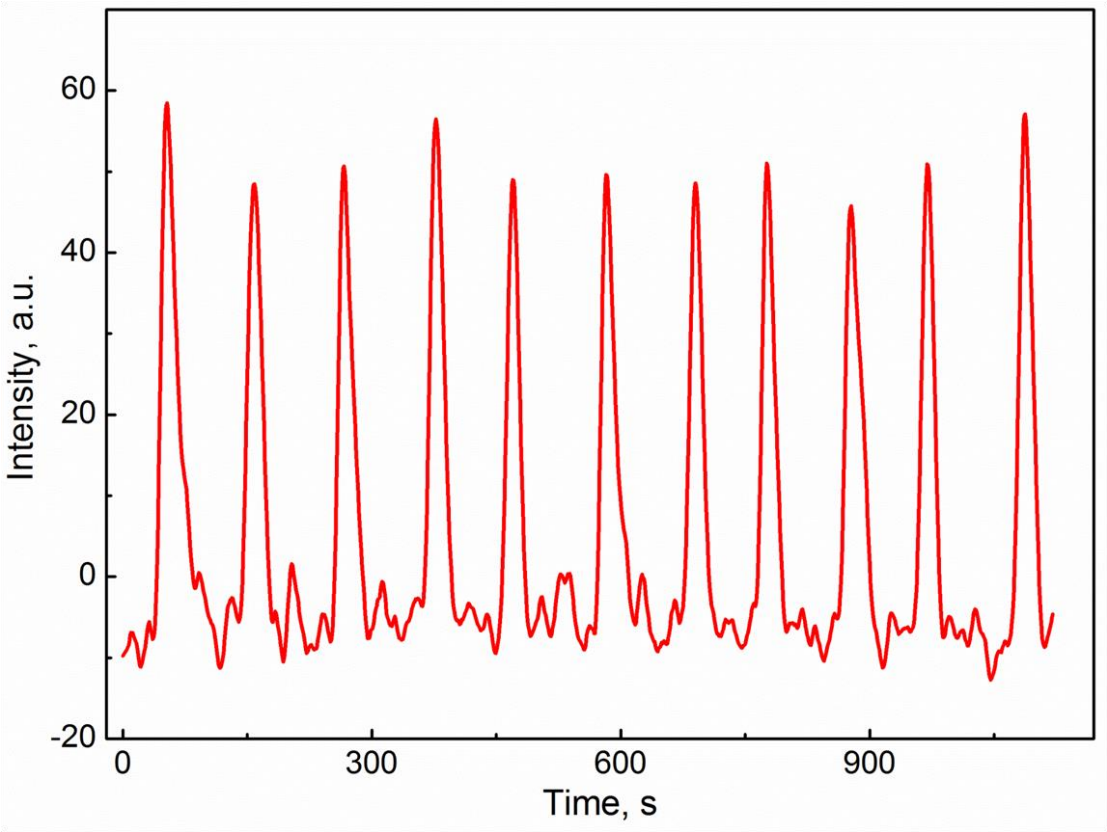

Figure S8. Temporal emission profile of 11 consecutive determinations of a 5 mg L^{-1} NPOC (as C) standard.

11. Comparison of Performance with Other Methods

Table S3. Comparison of Performance with Other Methods

Method	sample volume, mL	LOD, mg L^{-1}	Linear range, mg L^{-1}	Ref
Photo-oxidation-electrolytic conductivity	0.7 mL min^{-1}	0.002	0.002-4	1
Combustion, gravimetric method	100	5.0	10-1500	2
HTC-NDIR	0.06	0.036	0.24-6	3
HTC-ion chromatography	1000	0.002	0.01-2.5	4
direct ICP-AES	-	0.07	-	5
MOVG-DBD-AES	10	0.01	0.1-20	6
Conventional PVG-PD-OES	0.5	1	10-1000	This
HE-POVG-PD-OES	0.5	0.05	0.5-200	work

12. Calibration Curve Obtained by Using Continuous HE-POVG-PD-OES

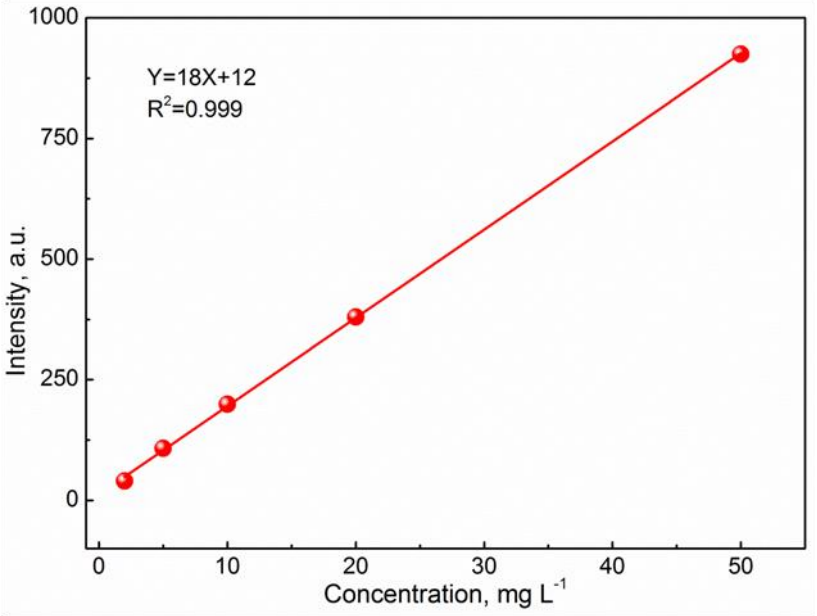

Figure S9. Calibration curve obtained by using Continuous HE-POVG-PD-OES

13. The Picture of Continuous and Continuous Monitoring of NPOC in Tap Water

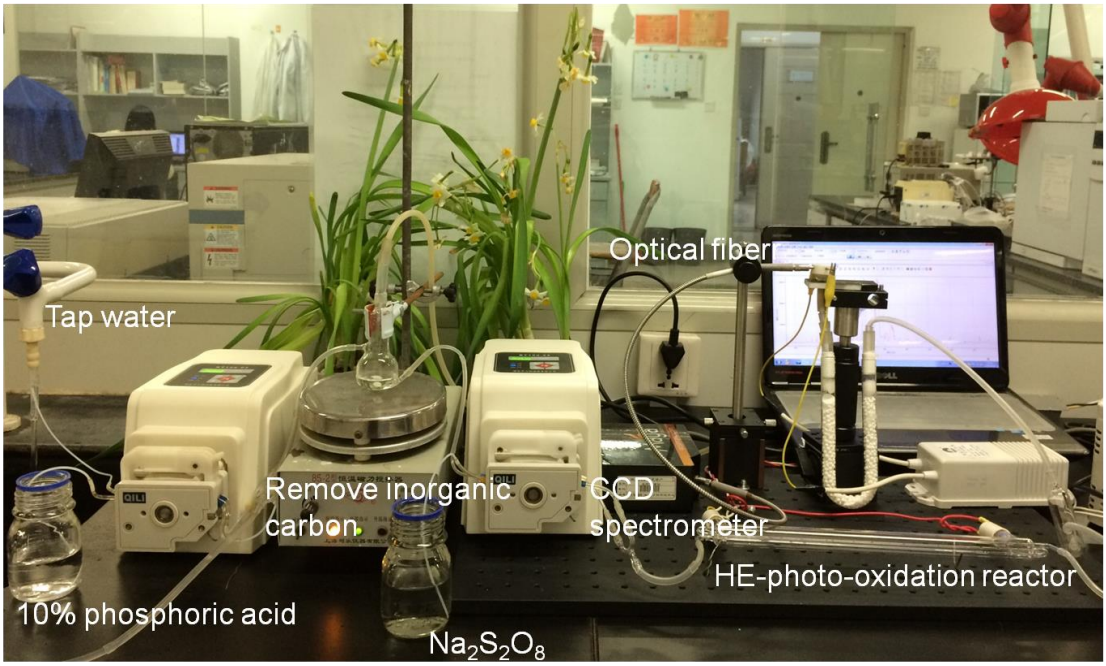

Figure S10. The picture of continuous and continuous monitoring of NPOC in tap water

Reference

1. Federer, U.; Kaufmann, P. R.; Hutterli, M. A.; Schupbach, S.; Stocker, T. F. Continuous flow analysis of total organic carbon in polar ice cores. *Environ. Sci. Technol.* **2008,** *42,* 8039-43.

2. Pickhardt, W. P.; Oemler, A. N.; Mitchell, J. Determination of total carbon in organic materials by wet-dry combustion method. *Anal. Chem.* **1955,** *27,* 1784−1788.

3. Qian, J. G.; Mopper, K. Automated high-performance, high-temperature combustion total organic carbon analyzer. *Anal. Chem.* **1996,** *68,* 3090–3097.

4. Fung, Y. S.; Wu, Z. C.; Dao, K. L. Determination of Total Organic Carbon in Water by Thermal Combustion-Ion Chromatography. *Anal. Chem.* **1996,** *68,* 2186−2190.

5. Maestre, S. E.; Mora, J.; Hernandis, V.; Todolí, J. L. A system for the direct determination of the nonvolatile organic carbon, dissolved organic carbon, and inorganic carbon in water samples through inductively coupled plasma atomic emission spectrometry. *Anal. Chem.* **2003,** *75,* 111−117.

6. Han, B. J.; Jiang, X. M.; Hou, X. D.; Zheng, C. B. Miniaturized dielectric barrier discharge carbon atomic emission spectrometry with online microwave-assisted oxidation for determination of total organic carbon. *Anal. Chem.* **2014,** *86,* 6214-6219.